ECCOMAS Congress 2016
VII European Congress on Computational Methods in Applied Sciences and Engineering
M. Papadrakakis, V. Papadopoulos, G. Stefanou, V. Plevris (eds.)
Crete Island, Greece, 5–10 June 2016

ALTERNATIVE TO RETURN-MAPPING ALGORITHM FOR COMPUTING PLASTIC STRAIN. APPLICATION TO DILATANT MATERIALS

Siegfried Maiolino[1,2]

[1]Cerema/DTerCE/DLL/RRMS–ER29
25, avenue Mitterrand
69674 Bron cedex France
e-mail: siegfried.maiolino@cerema.fr

[2] Laboratoire de Mécanique des Solides –UMR 7649
École Polytechnique
91128 Palaiseau cedex France

Keywords: Computing Methods, Elastoplasticity, Finite Element Methods, Numerical Methods, Geomechanics, Return Mapping

Abstract. *Computing plastic strain is a crucial issue in finite element methods. This problem is also known as closest point projection. The radial return used for circular models reduces the computations to literal expressions. But in geomechanics, the deviatoric shape of yield functions is generally non circular, so that return mapping algorithm becomes cumbersome and time consuming.*

Works that will be presented rather focus on a geometric based methods. It will be demonstrated that the numerical problem of closest point projection of the trial stress on the yield surface is equivalent to a geometrical bounded problem. Whereas this property is intuitive, the tools ensuring a straightforward equivalence between the two problems were to be developed.

We identify the geometric problem associated to the problem of the closest point projection in the deviatoric plane. The geometric problem is independent from the mechanical one, and can be solved with trigonometric and geometric laws. Those laws are integrated in a general algorithm to compute plastic strain, taking account of associated and non associated dilatancy for the computation of volumic plastic strains

1 INTRODUCTION

The Mohr'envelope of many porous media - soils, rocks, bones, compacted powder, show their dependence to mean stress, and also differences in strength between triaxial extension and traxial compression. Criteria like Coulomb or Hœk-Brown [3] take into account this dependence but present corners, whereas circular yield functions like Drucker-Prager don't. Experimental results using true triaxial tests prove that geomaterials present a triangular deviatoric shape with rounded corners [12]. Taking into account this particular shape in a smooth criterion involve using the third invariant. Various yield functions had been proposed, for soils [6, 11], concrete [16] or rocks [8].

The radial return [15] used for circular models reduces the computations to literal expressions [5]. The main drawback of non circular models is that return mapping algorithm becomes complex, expensive [13] and time consuming, even if efficiency is increased with spectral decomposition techniques [1, 2]. Works that will be presented rather focus on a geometric based methods : in order to bypass the computational costs of return mapping algorithm, we will focus on simpler equivalent geometric problems.

2 POLAR DECOMPOSITION OF THE YIELD SURFACE

Traction stresses are positive, and the principal stresses ordered as follow : $\sigma_I \geq \sigma_{II} \geq \sigma_{III}$

2.1 Geometric parametrage

For a given mean stress $\left(\sigma_m = \mathrm{Tr}\underline{\underline{\sigma}}/3\right)$, the yield surface can be reduced to its cross-sectional shape on the deviatoric plane, or π plane. A yield surface ($f\left(\underline{\underline{\sigma}}\right) = 0$) can be represented in a unique manner by the mean stress and the deviatoric invariants $\left(J_2 = \frac{1}{2}\mathrm{Tr}\left(\underline{\underline{s}}^2\right),\ J_3 = \frac{1}{3}\mathrm{Tr}\left(\underline{\underline{s}}^3\right)\right.$, with $\left.\underline{\underline{s}} = \underline{\underline{\sigma}} - \sigma_m\underline{\underline{\mathbb{1}}}\right)$, but it is more practical to replace the third invariant by the Lode angle θ, to work in the π plane (deviatoric plane).

$$-\frac{\pi}{6} \leq \theta = \frac{1}{3}\arcsin\left(\frac{-3\sqrt{3}}{2}\frac{J_3}{\sqrt{J_2}^3}\right) \leq \frac{\pi}{6} \tag{1}$$

The set $\left(\sqrt{J_2}, \theta\right)$ define polar coordinates on one sixth of the deviatoric plane, which is sufficient for an isotropic criterion. Zienkiewicz and Pande [17], using the fact that a yield surface can be reduced to its polar expression, provided tools to study the regularity, the sensitivity to the extension and the convexity of a criterion starting from the shape function $g_p\left(\theta\right)$

$$\sqrt{J_2} = \sigma^+ g_p\left(\theta\right) \tag{2}$$

The deviatoric radius : $\sigma^+(\sigma_m) = \sqrt{J_2}_{/\theta=\frac{\pi}{6}}$, gives the yield function in the meridional plane $\left(\sigma_m, \sqrt{J_2}\right)$, for $\theta = \frac{\pi}{6}$. This value of the Lode angle corresponds to a classical triaxial test, or compression triaxial test ($\sigma_I = \sigma_{II} > \sigma_{III}$). The function $g_p\left(\theta\right)$ is the shape function of the yield surface in the deviatoric plane. It is normalized $\left(g_p\left(\frac{\pi}{6}\right) = 1\right)$ and gives directly the value of the extension ratio $g_p\left(-\frac{\pi}{6}\right) = L_S$ which is more detailed in the following section.

2.2 Characteristic function of a material

The deviatoric radius σ^+ can be easily deduced from triaxial compression tests. Whether the shape is straight or parabolic, the deviatoric radius used can be the Coulomb or Hœk-Brown.

The extension ratio L_S has a physical meaning and can be determined from experiment. The condition $\theta = -\frac{\pi}{6}$ corresponds to extension triaxial tests ($\sigma_I > \sigma_{II} = \sigma_{III}$), which can be performed with the same triaxial cell as compression triaxial test.

$$L_S = \frac{\sqrt{J_2}\left(\theta = -\frac{\pi}{6}\right)}{\sqrt{J_2}\left(\theta = \frac{\pi}{6}\right)} = \frac{(\sigma_I - \sigma_{III})\,(extension)}{(\sigma_I - \sigma_{III})\,(compression)} \tag{3}$$

Physically, this means that for the same mean stress, the yield value of $\sqrt{J_2}$ would be lower in extension than in compression. The value of L_S is directly linked to the deviatoric shape of a yield surface. While this value can be independent from the mean stress (Coulomb), some rocks present a shape of their yield surface changing from triangular (low confinement) to circular (high confinement) [4], i.e, L_S increases from 0.5 to 1.

2.3 Introduction of the orthoradial tensor

We consider for stresses and strains (i.e. symetric second order tensors) the following scalar product. For two tensors, $\underline{\underline{T_1}}$ and $\underline{\underline{T_2}}$:

$$\underline{\underline{T_1}} \cdot \underline{\underline{T_2}} = \underline{\underline{T_1}} : \underline{\underline{T_2}} = \mathrm{Tr}\underline{\underline{T_1 T_2}} \tag{4}$$

Hence defining the following norm (Frobenius norm) for a symetric second order tensor $\underline{\underline{T}}$:

$$\| \underline{\underline{T}} \| = \sqrt{\underline{\underline{T}} : \underline{\underline{T}}} \tag{5}$$

We introduce the orthoradial tensor, $\underline{\underline{v}}$:

$$\underline{\underline{v}} = 3\frac{\sqrt{3}}{2}\frac{1}{J_2}\underline{\underline{s}}^2 - \sqrt{3}\underline{\underline{\mathbb{1}}} - \frac{9\sqrt{3}J_3}{4{J_2}^2}\underline{\underline{s}} \tag{6}$$

This tensor is orthoradial as $\underline{\underline{v}} \cdot \underline{\underline{\mathbb{1}}} = \underline{\underline{v}} \cdot \underline{\underline{s}} = 0$, hence those three tensors, $\underline{\underline{\mathbb{1}}}$, $\underline{\underline{s}}$, $\underline{\underline{v}}$ constitute an orthogonal basis of symetric second order tensors, for the Frobenius scalar product.

We can then easily decompose the derivatives of the yield function along this orthogonal basis, as the expression of the gradient of invariants can easily be expressed. It is necessary to introduce the orthogonal tensor, as the gradient of the third invariant cannot be expressed using only the hydrostatic tensor or the deviatoric tensor. Expressions of the three gradients of invariants using the orthogonal basis are the following :

$$\frac{\partial I_1}{\partial \underline{\underline{\sigma}}} = \underline{\underline{\mathbb{1}}} \tag{7}$$

$$\frac{\partial J_2}{\partial \underline{\underline{\sigma}}} = \underline{\underline{s}} \tag{8}$$

$$\frac{\partial J_3}{\partial \underline{\underline{\sigma}}} = \underline{\underline{s}}^2 - \frac{2J_2}{3}\underline{\underline{\mathbb{1}}} = \frac{3J_3}{2J_2}\underline{\underline{s}} + \frac{2J_2}{3\sqrt{3}}\underline{\underline{v}} \tag{9}$$

Hence the gradient of any yield surface can be orthogonally decomposed.

$$\frac{\partial f}{\partial \underline{\underline{\sigma}}} = f_u\underline{\underline{\mathbb{1}}} + f_s\underline{\underline{s}} + f_v\underline{\underline{v}} \tag{10}$$

We can observe that the deviatoric part of the gradient, $\frac{\partial f}{\partial \underline{\underline{\sigma}}}$ can be split in two orthogonal component, a radial $f_s\underline{\underline{s}}$, and a orthoradial, $f_v\underline{\underline{v}}$. This later part is null for criteria independent from the third invariant.

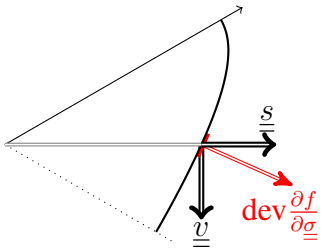

Figure 1: Otrthogonal decomposition of the deviatoric part of the gradient

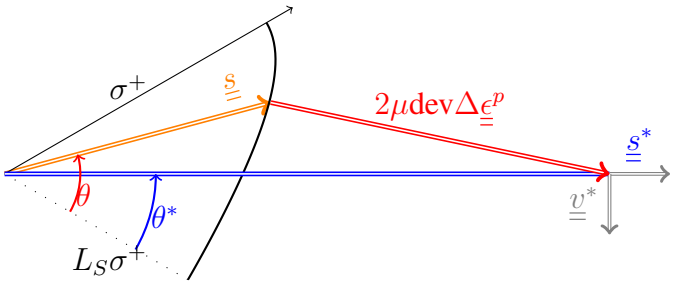

Figure 2: Physical problem in the deviatoric plane

2.4 Consequences for return mapping algorithm

Let us consider at an integration point, the increment from step n to $n+1$. We want to calculate the plastic strain, if the trial stress $\underline{\underline{\sigma}}^*$ doesn't satisfy the yield condition. We want to implicitly solve the relation that gives the stress.

$$\underline{\underline{\sigma}}_{n+1} = \underline{\underline{\sigma}} = \underline{\underline{\sigma}}^* - \underline{\underline{\underline{\underline{L}}}}\Delta\underline{\underline{\epsilon}}^p \tag{11}$$

Where $\underline{\underline{\underline{\underline{L}}}}$ is the elasticity tensor. We can split this relation between two orthogonal components : an hydrostatic and a deviatoric.

$$\sigma_m - \sigma_m^* = -K\text{Tr}\Delta\underline{\underline{\epsilon}}^p \tag{12}$$

$$\underline{\underline{s}} - \underline{\underline{s}}^* = -2\mu\text{dev}\Delta\underline{\underline{\epsilon}}^p \tag{13}$$

Where K is the bulk modulus and μ the shear modulus.

We can notice that the hydrostatic part (12) is purely scalar and that the main difficulties come from the deviatoric part(13).

3 GEOMETRIC EQUIVALENCE OF CLOSEST POINT PROJECTION

We introduce the following quantity [9, 10]:

$$\rho = \frac{\sqrt{J_2}^*}{\sigma^+(\sigma_m^* + \Delta\sigma_m)} \tag{14}$$

The closest point projection of $\underline{\underline{s}}^*$ on the trace of yield surface (Figure 2) is equivalent to the following geometric problem(Figure 3): find the closest point projection (polar coordinates:

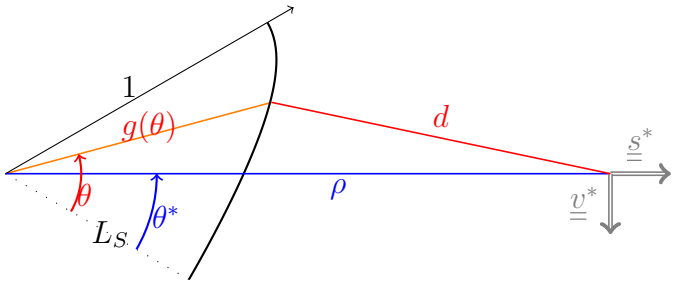

Figure 3: Geometric problem in polar coordinates

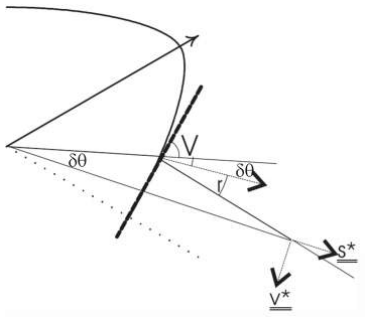

Figure 4: Angular relations: $V + r + \delta\theta = \frac{\pi}{2}, (\delta\theta = \theta - \theta^*)$

$(\theta, g_p(\theta)))$ of the point (ρ, θ^*) on the curve defined by the shape function $g_p(\theta)$. The function $d(\theta)$ reaches its minimum at this point.

$$d(\theta)^2 = g_p^2(\theta) + \rho^2 - 2g_p(\theta)\,\rho\cos(\theta - \theta^*) \tag{15}$$

The norm of the deviatoric plastic strain is given directly : $\| \text{dev}\Delta\underline{\underline{\epsilon}}^p \| = \frac{d(\theta)\sigma^+}{\sqrt{2}\mu}$, and $\text{dev}\Delta\underline{\underline{\epsilon}}^p$ can be written in the local base associated to the trial stress

$$\text{dev}\Delta\underline{\underline{\epsilon}}^p = \| \text{dev}\Delta\underline{\underline{\epsilon}}^p \| \left(\frac{\cos r}{\sqrt{2}\sqrt{J_2^*}}\underline{\underline{s}}^* + \frac{\sin r}{\| \underline{\underline{v}}^* \|}\underline{\underline{v}}^* \right) \tag{16}$$

The value of the r angle can be deduced from trigonometric considerations (figure 4), V being the angle between the tangent to a polar curve and the radial axis :

$$\tan V = \frac{g}{g'} \tag{17}$$

4 COMPUTATION OF DEVIATORIC AND HYDROSTATIC PLASTIC STRAIN

The geometric equivalence allows to get the plastic strain if $\Delta\sigma_m$ is known. This quantity is calculated using an iterative method. Initially, $\Delta\sigma_m^0 = 0$, and the stopping condition c is satisfied when the ratio between hydrostatic and deviatoric parts is equal to the dilatancy angle δ.

$$c(\Delta\sigma_m, \| \text{dev}\Delta\underline{\underline{\epsilon}}^p \|, \tan\delta) = \| \text{dev}\Delta\underline{\underline{\epsilon}}^p \| + \frac{\Delta\sigma_m}{\sqrt{3}K\tan\delta} < \varepsilon \tag{18}$$

We use the following definition of the dilatancy angle :

$$\tan\delta = -\frac{\mu_l}{\sqrt{2}}\frac{\partial\epsilon_V^p}{\partial\epsilon_d^p} \tag{19}$$

Where ϵ_V^p is the volumic plastic strain, and $\mu_l = \tan 3\theta$ the factor initially defined by Lode [7]. Using the Lode factor allows to use a formulation that can be used for triaxial compression test as well as extenions test [14].

The dilatancy angle can be deduced from the expression of the yield function (associated potential) or from a non associated potential. Whereas it is not easy to identify the potential, without extensive true trixial tests, the dilatancy angle can be easily identified using classical triaxial compression tests.

If $\delta > 0$ material is said to be dilatant. The alternative return mapping algorithm can be expressed as follow, at a given integration point, for a dilatant material

1. Compute $\underline{\underline{\sigma}}^* = \underline{\underline{\sigma}}^0 + \underline{\underline{\underline{\underline{L}}}} \left(\underline{\underline{\epsilon}}_{n+1} - \underline{\underline{\epsilon}}_n^p \right)$
2. Check $f(\underline{\underline{\sigma}}^*) > 0$? No set $\underline{\underline{\sigma}}_{n+1} = \underline{\underline{\sigma}}^*$ and exit.
3. Yes : set i = 0 and $\Delta\sigma_m^0 = 0$
4. Set $\rho^i = \frac{\sqrt{J_2^*}}{\sigma^+(\sigma_m^* + \Delta\sigma_m^i)}$ and if L_S depends of mean stress : $L_S^i = L_S\left(\sigma_m^* + \Delta\sigma_m^i\right)$
5. Compute θ^i, $d\left(\theta^i\right)$, $\sqrt{J_2}^i$ and $\parallel \text{dev}\Delta\underline{\underline{\epsilon}}^p \parallel^i$
6. Evaluate $\tan\delta^i = \tan\delta\left(\sigma_m^* + \Delta\sigma_m^i, J_2^i, J_3^i\right)$
7. Evaluate stopping criterion $\mid c\left(\sigma_m^* + \Delta\sigma_m^i, \parallel \text{dev}\Delta\underline{\underline{\epsilon}}^p \parallel^i, \tan\delta^i\right) \mid < \epsilon$. If Yes compute angle r and tensor $\Delta\underline{\underline{\epsilon}}^p$. Update $\underline{\underline{\sigma}}_{n+1} = \underline{\underline{\sigma}}^* - \underline{\underline{\underline{\underline{L}}}}\Delta\underline{\underline{\epsilon}}^p$ and exit.
8. If No, set $i = i + 1$ and $\Delta\sigma_m^i = \Delta\sigma_m^{i-1} + \Delta^2\sigma_m$, then loop to step 4.

The evaluation of $\Delta^2\sigma_m$ depends of the nature of yield function f and δ

5 CONCLUSIONS

We have shown that for J_3 dependant yield function, the problem of closest point projection is equivalent to a pure geometric problem in polar coordinates. For different values of (ρ, θ^*), solutions can be computed and values of $d\left(\theta\right)\sin 3\theta$ and $g_p\left(\theta\right)$ are saved, allowing to short-cut computational costs of return mapping in the deviatoric plane. For the hydrostatic part, we propose a general algorithm that allows to take account of the dilatancy in the computation of plastic strain. Next step will be to define the stability conditions for negative dilatancy (i.e. contractant material). The last wil be to extend the process to non associated plasticity in the deviatoric plane. References and experimental studies of non associated flow rules in the deviatoric part are scarce, so many cases must be considered.

References

[1] R. Borja, K. Sama, and P. Sanz. On the numerical integration of three invariant elasto-plastic constitutive models. *Comput. Methods Appl. Mech. Engrg*, 192(9-10):1227–1258, 2003.

[2] C. Foster, R. Regueiro, A. Fossum, and R. Borja. Implicit numerical integration of a three-invariant, isotropic/kinematic hardening cap plasticity model for geomaterials. *Comput. Methods Appl. Mech. Engrg.*, 194(50-52):5109–5138, 2005.

[3] E. Hoek and E. Brown. Empirical strength criterion for rock masses. *J. Geotech. Engng DIV., ASCE*, 106(GT9):1013–1035, 1980.

[4] M. Kim and P. Lade. Modelling rock strength in three dimensions. *Int. Journ. Rock Mech. Min. Sci. Abstracts*, 21(1):21–33, 1984.

[5] R. D. Krieg and S. M. Key. Implementation of a Time Dependant Plasticity Theory into Structural Computer Programs. *Constitutive Equations in Viscoplasticity : Computational and Engineering Aspects*, 20:125–137, 1976.

[6] P. V. Lade. Elasto-plastic stress-strain theory for cohesionless soil with curved yield surfaces. *Int. Journ. Solids Structures*, 13:1019–1035, 1977.

[7] W. Lode. Versuche über den Einfluß der mittleren Hauptspannung auf das Fließen der Metalle Eisen, Kupfer und Nickel. *Zeitschrift für Physik*, 36:913–939, 1926.

[8] S. Maïolino. Proposition of a general yield function in geomechanics. *Comptes Rendus Mécanique*, 333:279–284, 2005.

[9] S. Maïolino. *Fonction de charge générale en géomécanique : application aux travaux souterrains*. PhD thesis, École Polytechnique, 2006. General yield function in geomechanics : application to tunneling (in French).

[10] S. Maïolino. Numerical abacuses method based on the equivalence between the closest point projection and a bounded geometric problem. In *8th.World Congress on Computational Mechanics (WCCM8) , 5th European Congress on Computational Methods in Applied Sciences and Engineeering (ECCOMAS 2008), Venice*, July 2008.

[11] H. Matsuoka and T. Nakai. Stress-deformation and strength characteristics of soil under three different principal stresses. In *Proc. JSCE*, volume 232, pages 59–70, 1974.

[12] P. Michelis. True triaxial yelding and hardening of rock. *J. Geotech. Engng DIV., ASCE*, 113(6):616–635, 1987.

[13] J. Simo and T. Hughes. *Computational Inelasticity*. 1998.

[14] L. Thorel. *Plasticité et endommagement des roches ductiles - application au sel gemme.* PhD thesis, 1994.

[15] J. L. Wilkins. Calculation of Elastic-plastic Flow. *Methods of Compuational Physics*, 8, 1964.

[16] K. William and E. Warnke. Constitutive models for the triaxial behavior of concrete. In *International Association of Bridge and Structural Engineering (IABSE) Seminar on "Concrete Structures Subjected to Triaxial Stresses", Bergamo*, volume 19, pages 1–30, 1975.

[17] O. C. Zienkiewicz and G. N. Pande. Some useful forms of isotropic yeld surfaces for soil and rock mechanics. In *Numerical methods in soil and rock mechanics, Karlsruhe*, pages 3–16, september 1975.